Published in final edited form as:
J Neurosci. 2005 October 26; 25(43): 9940–9948. doi:10.1523/JNEUROSCI.3467-05.2005.

Vascular Development of the Brain Requires β8 Integrin Expression in the Neuroepithelium

John M. Proctor[1], **Keling Zang**[1], **Denan Wang**[1], **Rong Wang**[2], and **Louis F. Reichardt**[1]

[1]Howard Hughes Medical Institute and Department of Physiology, University of California, San Francisco, California 94143

[2]Department of Surgery, University of California, San Francisco, California 94143

Abstract

We showed previously that loss of the integrin β8 subunit, which forms αvβ8 heterodimers, results in abnormal vascular development in the yolk sac, placenta, and brain. Animals lacking the integrin β8 (*itgβ8*) gene die either at midgestation, because of insufficient vascularization of the placenta and yolk sac, or shortly after birth with severe intracerebral hemorrhage. To specifically focus on the role of integrins containing the β8 subunit in the brain, and to avoid early lethalities, we used a targeted deletion strategy to delete *itgβ8* only from cell types within the brain. Ablating *itgβ8* from vascular endothelial cells or from migrating neurons did not result in cerebral hemorrhage. Targeted deletion of *itgβ8* from the neuroepithelium, however, resulted in bilateral hemorrhage at postnatal day 0, although the phenotype was less severe than in *itgβ8*-null animals. Newborn mice lacking *itgβ8* from the neuroepithelium had hemorrhages in the cortex, ganglionic eminence, and thalamus, as well as abnormal vascular morphogenesis, and disorganized glia. Interestingly, adult mice lacking *itgβ8* from cells derived from the neuroepithelium did not show signs of hemorrhage. We propose that defective association between vascular endothelial cells and glia lacking *itgβ8* is responsible for the leaky vasculature seen during development but that an unidentified compensatory mechanism repairs the vasculature after birth.

Keywords

brain; cortex; hemorrhage; integrin; neuroepithelium; vasculature

Introduction

Vascular development of the CNS depends on cells within the brain that secrete factors, such as vascular endothelial growth factor (VEGF), which promote and guide capillary growth (Ruhrberg et al., 2002; Gerhardt et al., 2003). To fully appreciate the complexity of vascular development within the CNS, however, requires a better understanding of the molecules used for endothelial cell and neuroepithelial cell communication. These complex interactions between endothelial cells of the vasculature and neuroepithelial cells are also essential for formation of the blood–brain barrier (BBB), which is important for homeostatic regulation of the brain microenvironment and is necessary for development and healthy function of the CNS (Abbott and Romero, 1996; Engelhardt, 2003).

Correspondence should be addressed to Louis F. Reichardt, Howard Hughes Medical Institute, University of California, San Francisco, Department of Physiology, 1550 4th Street, Room 284A, San Francisco, CA 94143-2611. E-mail: lfr@cgl.ucsf.edu.

Vascular development within the CNS is regulated by cell–matrix and cell– cell interactions. Integrins are important heterodimeric extracellular matrix (ECM) receptors that mediate cell adhesion, cell migration, and tissue organization (Calderwood, 2004). Several molecules have been identified that function during vasculogenesis and development of the BBB (Engelhardt, 2003; Park et al., 2003), but only integrins containing either the αv or β8 subunits have been shown to be required for proper capillary development within the CNS (Bader et al., 1998; McCarty et al., 2002, 2005; Zhu et al., 2002). The αv integrin subunit is the only known partner for β8, and the integrin αvβ8 has been shown to bind the latency-associated peptide of TGF-β1 and vitronectin (Moyle et al., 1991; Nishimura et al., 1994; Mu et al., 2002). Other evidence suggests αvβ8 may also bind laminin and collagen IV (Venstrom and Reichardt, 1995).

Deletion of the integrin β8 (*itgβ8*) gene during development results in severe cerebral hemorrhage, with death of null mice occurring during embryogenesis or shortly after birth (Zhu et al., 2002). Similarly, deletion of integrin αv (*itgαv*) also results in severe cerebral hemorrhage and neonatal death (Bader et al., 1998; McCarty et al., 2002). In addition to the β8 subunit, αv can associate with several other β subunits including β1, β3, β5, and β6. These subunits, however, are not likely to be essential in vascular development of the neuroepithelium, because no vascular defects were observed in *itgβ3/itgβ5* double knock-out mice or *itgβ6* mutants (Huang et al., 1996; McCarty et al., 2002). Furthermore, no cerebral hemorrhage has been observed in mice lacking *itgβ1* in neuroepithelial cells (Graus-Porta et al., 2001). This evidence strongly suggests that αv and β8 function together as a heterodimer in the CNS during vasculogenesis.

To determine the cellular basis for the cerebral hemorrhage observed in *itgβ8*-null neonates, we generated a conditional *itgβ8* knock-out mouse (*itgβ8* flox). Using these mice, we selectively ablated *itgβ8* from neuroepithelial cells, endothelial cells, and migrating neurons. Whereas deletion of *itgβ8* from the neuroepithelium results in intracerebral hemorrhage, deletion from endothelial cells or from neurons does not. Tissue-specific deletion of *itgβ8* from the neuroepithelium also resulted in morphologically abnormal capillaries and disorganized astroglial cells. Therefore, the presence of integrins containing the β8 subunit on neuroepithelial-derived glial cells is essential for proper regulation of vascular morphogenesis in the developing CNS.

Materials and Methods

Generation of "floxed" *itgβ8* mice

Using standard procedures, the targeting construct was generated by inserting a phosphoglycerate kinase–neomycin (PGK-neo) cassette, flanked by *frt* sites and containing one loxP site at its 3′ terminus, into the *Eco*RV restriction site between exons 4 and 5 in a genomic fragment of *itgβ8* containing exons 4, 5, and 6. A second loxP site was inserted into the intron between exons 3 and 4. The targeted allele was subsequently generated via homologous recombination by introducing the linearized targeting construct into undifferentiated SVJ129 mouse embryonic stem (ES) cells using standard methods.A 5′ 670 bp and a 3′ 700 bp genomic DNA fragment of *itgβ8* were used as probes for Southern blot identification of ES cells containing the targeted allele. Four independently targeted ES cell clones were identified. Two clones were injected into C57BL/6J blastocysts and then placed in pseudopregnant C57BL/6J females. One gave germline transmission, which was confirmed by Southern blot. Chimeric mice carrying the floxed *itgβ8* allele were crossed to C57BL/6J mice. The progeny of that cross was crossed to mice carrying the enhanced *flp* recombinase gene (*flpE*) under the control of the ubiquitous β-actin promoter (Rodriguez et al., 2000) to remove the PGK-neo cassette. These mice were then interbred to obtain $itg\beta8^{flox/flox}$ mice. Total RNA for Northern blots was obtained from control and mutant β-*actin-cre itgβ8* postnatal day 0 (P0) brains using the Qiagen (Valencia, CA) RNeasy Mini kit. A 700 bp fragment from

the 3′ untranslated region of *itgβ8* was used as a probe. A 500 bp fragment of the *GAPDH* (glyceraldehyde-3-phosphate dehydrogenase) gene was used as a probe as a control for RNA load.

PCR genotyping of mice

Female *itgβ8*$^{flox/flox}$ mice were crossed to male *itgβ8*$^{null/+}$;cre/+ mice to generate *itgβ8*$^{flox/null}$;*cre*/+mutant progeny, as well as heterozygous and wild-type littermate progeny. All progeny were genotyped by standard PCR analysis using DNA from tail tissue. Primers specific for each allele were used to identify progeny and are as follows: *itgβ8* wild-type (250 bp) and floxed allele (370 bp) (5′-GAGATGCAAGAGTGTTTACC-3′) and (5′-CACTTTAGTATGCTAATGATGG-3′); *itgβ8*-null allele (450 bp) (5′-AGAGGCCACTTGTGTAGCGCCAAG-3′) and (5′-GGAGGCATACAGTCTAAATTGT-3′); cre (400 bp) (5′-CTGGCAATTTCGGCTATACGTAACAGGGTG-3′) and (5′-GCCTGCATTACCGGTCGATGCAAC-3′).

Mouse lines

The β-*actin-flpE* mice (Rodriguez et al., 2000), the *nestincre* mice (Tronche et al., 1999), and the *nescre8* mice (Petersen et al., 2002) have been described previously. The *tie2-cre* mice were generously provided by R. Wang [University of California, San Francisco (UCSF), San Francisco, CA] (R. Braren and R. Wang, unpublished observations). The *nex-cre* mice have been described previously (Beggs et al., 2003; Brockschnieder et al., 2004) but were kindly provided before publication by K. A. Nave (Max-Planck Institute, Göttingen, Germany). The β-*actincre* mice were generously provided by G. Martin (UCSF) and have been described previously (Lewandoski et al., 1997). Mice were cared for according to animal protocols approved by the UCSF Committee on Animal Research.

Morphological and histological analysis

Whole brains, dissected from P0 mice, were photographed using a CCD camera mounted on a dissecting microscope. Brains were then submerged in 4% paraformaldehyde in PBS overnight at 4°C, followed by submersion in 30% sucrose at 4°C until saturated, and then frozen in Tissue-Tek OCT (Miles, Elkhart, IN) for cutting 20 μm sections using a cryostat. Embryos used for immuno-histochemistry were decapitated, and the heads were then fixed in 4% paraformaldehyde in PBS for 1–2 h, cryoprotected in 30% sucrose, embedded in OCT, and cut on the cryostat (20 μm sections). For LacZ staining, whole embryos or P0 brains were fixed for 2 h in 0.2% glutaraldehyde at 4°C, washed in PBS containing 0.02% NP-40 for 15 min, and stained with a freshly made X-gal (5-bromo-4-chloro-3-indolyl-β-D-galactopyranoside) solution according to the standard protocol. These embryos were subsequently fixed in 4% paraformaldehyde in PBS overnight, cryoprotected in 30% sucrose, embedded in OCT, and cut on the cryostat (15 μm sections). All sections were counterstained with Nuclear Fast Red according to a standard protocol. Adult mice were anesthetized with 2.5% avertin in 0.9% NaCl, using 15 μl per gram of mouse weight and perfused with 4% paraformaldehyde in PBS. This tissue was frozen directly in 30% sucrose for cutting 40 μm sections using a sliding microtome. Nissl stain was used according to standard procedures.

Immunohistochemistry

The following primary antibodies were used: GFAP polyclonal antibody (pAb) (1:250; Dako, High Wycombe, UK), platelet–endothelial cell adhesion molecule (PECAM) (CD31) monoclonal antibody (mAb) (1:150; PharMingen, San Diego, CA), RC2 mAb (1:4; Hybridoma Bank, Iowa City, IA), collagen IV pAb (1:1000; Cosmo Bio, Tokyo, Japan), Englebreth–Holm–Swarm laminin pAb (1:3000; Sigma, St. Louis, MO), α-smooth muscle actin mAb

(1:500; Sigma), and β-galactosidase (1:5000; ICN Biochemicals, Costa Mesa, CA). All sections stained with the RC2 monoclonal antibody were subjected to heat-based antigen retrieval in 10 mM sodium citrate buffer, pH 6.0, using the 34700 BioWave Microwave (Ted Pella, Redding, CA). OCT embedded frozen sections were placed in 5% goat serum, 5% BSA, and 0.3% Triton X-100 for 2 h at room temperature. Sections were incubated with primary antibodies overnight at 4°C, followed by fluorescent labeling with mouse or rabbit Alexa 488 (1:250; Invitrogen, Eugene, OR) or Texas Red (1:500; Invitrogen) in blocking buffer. For the isolectin B4 staining, paraformaldehyde-fixed sections were blocked as above for primary antibodies, followed by permeabilization in PBS containing 1% Triton X-100, 1 mM $CaCl_2$, 1 mM $MgCl_2$, and 0.1 mM $MnCl_2$. These sections were then incubated with biotin-conjugated isolectin B4 (20 ng/μl; L-2140; Sigma) overnight at 4°C in permeabilization solution. After five washes in PBS, sections were incubated with streptavidin-conjugated Alexa 594 (1:500; Invitrogen) in blocking buffer. Some sections were counterstained with the nuclear marker TO-PRO-3 (1:4000; Invitrogen). All sections were analyzed using a Zeiss LSM 5 Pascal confocal microscope. Radial glia morphology near the pial surface was analyzed by first collecting a z-series of images and then, using the Pascal program, collapsing the images into one projection image.

Results

Targeting strategy for conditional inactivation of the *itgβ8* gene

In a previous study, we observed that two-thirds of *itgβ8*-null mutant homozygotes die during midgestation because of defects in vascularization of the yolk sac and placenta. In the remaining one-third, *itgβ8*-null mice were born with severe cerebral hemorrhages and died shortly after birth (Zhu et al., 2002). To gain a better understanding of the cell types responsible for the cerebral hemorrhage in the *itgβ8*-null mutant, we generated a conditional floxed allele of *itgβ8* using cre/loxP technology. The *itgβ8* locus was targeted in ES cells using a construct containing loxP sites flanking exon 4 and a PGK-neo selection cassette inserted into the intron between exons 4 and 5 (supplemental Fig. 1*A*, available at www.jneurosci.org as supplemental material). Exon 4 encodes the integrin I-like domain, which has been shown to contribute to ligand binding in other integrin heterodimers (Tuckwell and Humphries, 1997; Green et al., 1998; Xiong et al., 2001). Cre-mediated deletion of exon 4 results in a translational frameshift that generates a premature stop codon. As a result, *itgβ8* mRNA is destabilized by the mRNA surveillance mechanism that degrades mRNA containing untranslated exons (Mendell et al., 2004). Thus, there is no detectable mRNA expressed in recombined cells, as assessed by Northern blot (supplemental Fig. 1*C*, available at www.jneurosci.org as supplemental material). This is consistent with our previous observation that disruption of exon 4, in *itgβ8*-null animals, leads to a lack of *itgβ8* mRNA expression (Zhu et al., 2002). Therefore, we predict that there are no functional αvβ8 heterodimers expressed by mutant cells in *itgβ8* conditional mutants. Homozygous $itgβ8^{flox/flox}$ mice were viable, fertile, and showed no obvious phenotype.

Loss of *itgβ8* from neuroepithelial cells results in cerebral hemorrhage

Integrin αvβ8 is expressed in neurons and glia in the mouse CNS (Milner et al., 1997; Nishimura et al., 1998). Although *itgαv* and *itgβ8* mRNA are both strongly expressed in neuroepithelial cells, neither has been detected on the endothelial cells of the vasculature (Pinkstaff et al., 1999; Zhu et al., 2002). Nevertheless, it remained possible that undetectable amounts of *itgβ8* expression in the CNS vasculature could contribute to the hemorrhagic phenotype in mice resulting from complete deletion of *itgβ8*. To determine which cell types were responsible for the hemorrhage observed in *itgβ8*-null animals, *itgβ8* was separately ablated from neuroepithelial cells, endothelial cells, and cortical neurons. Deletion of *itgβ8* was accomplished by crossing female $itgβ8^{flox/flox}$ mice with male $itgβ8^{null/+}$ mice expressing cre-

recombinase in the specified cell type (supplemental Fig. 1*D*, available at www.jneurosci.org as supplemental material), resulting in mutant animals hemizygous for the *cre* transgene and carrying one *itgβ8*-floxed allele and one *itgβ8*-null allele.

To address the hypothesis that *itgβ8* expression in neuroepithelial cells is necessary for proper vascular morphogenesis in the mouse brain, we first ablated *itgβ8* specifically from the neuroepithelium using a *nestin-cre* transgenic mouse line, which expresses cre under the control of the neural enhancer element of the *nestin* promoter (Tronche et al., 1999). Because only the neural enhancer element, and not the entirety of the *nestin* promoter–enhancer region, is used to drive *cre* expression, not all cells that express *nestin* endogenously express *cre*. It has been reported that neural precursor cells that give rise to both neurons and glia are recombined as early as embryonic day 10.5 (E10.5) using this *nestin-cre* transgene and that endothelial cells remain unrecombined (Graus-Porta et al., 2001). In contrast to a control animal (Fig. 1*A*), examination of whole brains from P0 mice demonstrated that excision of *itgβ8* from the neuroepithelium using *nestin-cre* results in cerebral hemorrhage (n=6) (Fig. 1*D*). All mutant animals observed had bilateral hemorrhages distributed across their cortices. Brain morphology in coronal sections was examined using both Nissl (Fig. 1) and hematoxylin and eosin staining (data not shown). We found that 100% of *nestin-cre* mutant brains had visible hemorrhages throughout the dorsal cortex (Fig. 1*E*), as well as large hemorrhages present within the thalamus (Fig. 1*F*) and in the ganglionic eminence near the deep mesencephalic nucleus (data not shown). This phenotype is less severe and less widespread across the cortex than that observed in the *itgβ8*-null animals (Fig. 1*G*). The reduced severity of the hemorrhagic phenotype using this *nestin-cre* line may be attributable to incomplete recombination of the neuroepithelium. To address this possibility, we crossed the *nestin-cre* line with the R26R reporter strain and collected embryos at E15, just one-half day after the onset of hemorrhage in this mutant (Fig. 1*H*). Recombination appeared complete throughout the cortex and ganglionic eminence (Fig. 1*I*), and no β-galactosidase was detected in endothelial cells (Fig. 1*J–L′*) or vascular smooth-muscle cells (supplemental Fig. 2, available at www.jneurosci.org as supplemental material).

A second explanation for the reduction in severity of hemorrhage seen in the *nestin-cre* mutants may be the perdurance of a small amount of *itgβ8* mRNA produced before deletion of *itgβ8* by *nestin-cre*. Because expression of this transgene begins at E10.5 (Graus-Porta et al., 2001), we used the *nescre8* transgenic mouse line, which expresses *cre* under control of the entire *nestin* promoter/enhancer beginning at E8.5 (Petersen et al., 2002). Hemorrhages in these mutants appeared by day E12.5 (supplemental Fig. 3*B*, available at www.jneurosci.org as supplemental material), the same time at which *itgβ8*-null animals develop intracerebral hemorrhage, but 2 d earlier than observed using the *nestin-cre* line. However, all *nescre8* mutants observed at P0 had hemorrhages more similar to those obtained using *nestin-cre* than those seen in the *itgβ8*-null animal (n = 5) (supplemental Fig. 3*C*, available at www.jneurosci.org as supplemental material), suggesting that factors in addition to loss of *itgβ8* in the neuroepithelium contribute to the more severe hemorrhage observed in *itgβ8*-null animals.

To determine whether integrin β8 expressed in endothelial cells is also necessary for normal development of brain vasculature, we ablated *itgβ8* specifically from endothelial cells using *cre* driven by the *tie2* promoter (Fig. 2). This transgene drives *cre* expression in most endothelial cells by E7.5 (R. Braren and R. Wang, unpublished observations). By E9, *tie2*-driven *cre* expression is very strong in the head vasculature before invasion of the neuroepithelium (Fig. 2*E–F*). Mutants generated using the *tie2-cre* transgene showed no sign of hemorrhage in the cortex or thalamus, nor were other brain defects observed (n = 7) (Fig. 2*G–I*). These data indicate that loss of αvβ8 protein from endothelial cells does not account for the hemorrhagic phenotype observed in *itgβ8 nestin-cre* mutants or *itgβ8*-null animals.

To determine whether absence of *itgβ8* from cortical neurons contributed to the hemorrhage defect seen in *itgβ8*-null animals, *nex-cre* (Beggs et al., 2003; Brockschnieder et al., 2004) was used to delete *itgβ8* from those cells (Fig. 3). The *cre* cDNA was inserted using a knock-in strategy into the *nex* locus, ensuring *nex* cell-specific expression of *cre* (Brockschnieder et al., 2004). This basic helix-loop-helix transcription factor drives *cre* expression primarily in pyramidal, postmitotic migrating neurons in the future cortical plate by E11, with robust expression throughout the forebrain by E12.5 (S. Goebbels and K. Nave, unpublished observations). When $itg\beta8^{flox/flox}$ animals were crossed to $itg\beta8^{null/+}$;*nex-cre*/+ mice, mutant progeny showed no sign of cerebral hemorrhage or other brain defects ($n = 3$) (Fig. 3*A–C*), indicating that expression of β8 in cortical neurons is not necessary for proper vascular morphogenesis in the CNS.

Together, these data indicate that *itgβ8* in the neuroepithelium is essential for proper vascular formation during development. Deletion of *itgβ8* specifically from endothelial cells or from migrating cortical neurons does not result in hemorrhage. Additionally, deletion of *itgβ8* specifically from cells in the neuroepithelium using *nestin-cre* or *nescre8* does result in cerebral hemorrhage during development that closely resembles, but is less severe than, the hemorrhage identified in the complete *itgβ8*-null mice (Zhu et al., 2002).

Loss of *itgβ8* in neuroepithelial cells results in endothelial cell abnormalities in the developing cortex

To further characterize the nature of the defect observed in the *itgβ8 nestin-cre* mutants, we used confocal microscopy to visualize cortical vasculature in coronal sections of the cortex by immunostaining with an antibody recognizing PECAM, a membrane glycoprotein expressed on the surface of endothelial cells. During development, a uniformly sized, primary capillary plexus is formed in the neural tube through angiogenesis (Yancopoulos et al., 2000). Anti-PECAM immunostaining of endothelial cells in sections of the forebrain from control mice labels this uniform plexus at P0 (Fig. 4*A,B*). A normal plexus also developed in mice from which *itgβ8* had been deleted in endothelial cells using *tie2-cre* (Fig. 4*K,L*). However, deletion of *itgβ8* from the neuroepithelium using *nestin-cre* resulted in vessels with large irregular endothelial cell clusters (Fig. 4*F,G*). These clusters are similar to those observed in *itgβ8*-null embryonic neuroepithelium (Zhu et al., 2002). We hypothesize that these abnormal clusters of endothelial cells may reflect aberrant endothelial cell migration or hyperproliferation during development of the brain and may permit leakage and subsequent hemorrhage of the vasculature.

The presence of endothelial cell clusters in *nestin-cre* mutant vessels suggested that improper basement membrane deposition or organization could result in the improper clustering of endothelial cells. However, anti-collagen IV immunostaining of the basement membrane of vessels in the cortex was normal in the *itgβ8 nestin-cre* mutants, even in areas of bulbous endothelial cell clusters (Fig. 4*H,J*). Anti-laminin immunostaining of the vessel basement membranes also appeared normal in the *itgβ8 nestincre* mutants compared with control animals (data not shown). This confirms our previous finding in the *itgβ8*-null animals that loss of *itgβ8* does not cause a general defect in basement membrane assembly, although discontinuities were observed possibly because of secondary effects of hemorrhage (Zhu et al., 2002).

Pericytes also appeared to be recruited normally to endothelial cells in *nestin-cre* mutant brains as detected by anti-α-smooth-muscle-actin immunostaining (Fig. 4*I,J*). Pericytes were recruited to both stalk cells of the vessels and cells within the bulbous endothelial cell clusters. This finding is consistent with the normal recruitment of pericytes we reported previously in the *itgβ8*-null animals (Zhu et al., 2002).

Conditional deletion of *itgβ8* from the neuroepithelium results in glial disorganization in the mouse brain

The known juxtaposition of glial cells and endothelial cells in the brain (Kacem et al., 1998; Simard et al., 2003) suggested that a primary defect in glial cells could give rise to a secondary endothelial cell phenotype in the *itgβ8 nestin-cre* mutant. Using confocal microscopy, we examined astroglia and radial glia in control and *itgβ8 nestin-cre* mutant P0 cortices. Cortical astroglial processes in wild-type P0 neonates were arrayed in a very regular pattern and were parallel to and in close association with blood vessels (Fig. 5*A*,*A′*). In a matched section from an *itgβ8 nestin-cre* mutant, astroglia appeared disorganized. They did not have the regular parallel organization seen in the control. Furthermore, in contrast to the wild type, blood vessels in the mutant did not run parallel to these glial processes (Fig. 5*E*,*E′*). The lack of alignment of the blood vessels and astroglial processes observed in the *itgβ8 nestin-cre* mutant may be explained by our previous observation that endothelial cells in the *itgβ8*-null mice were not well attached to the surrounding brain parenchyma, as observed by electron microscopy (Zhu et al., 2002).

Radial glia are precursor cells that give rise to both neurons and glial cell types (Doetsch, 2003) and have been shown to express αv integrins (Hirsch et al., 1994). To examine whether radial glia were also disorganized in the *nestin-cre* mutant, we stained E14.5 coronal forebrain sections for RC2, an early radial glia marker (Misson et al., 1988). E14.5 corresponds to the earliest time that hemorrhage was observed in the *nestin-cre* mutants. Control animals showed the expected radial pattern of glia in the ganglionic eminence of the neuroepithelium (Fig. 5*B*). However, in the *itgβ8 nestin-cre* mutants, radial glia were very disorganized in the ganglionic eminence (Fig. 5*F*). Because all nestin-cre mutants had visible hemorrhage in the ganglionic eminence at this time, we looked in areas of the developing cortex where hemorrhage had not yet occurred. Radial glial processes appeared normal and pial attachment did not appear altered in the *nestin-cre* mutants (Fig. 5*G*,*H*). These data suggest that radial glial disorganization closely coincides with, but may be a secondary consequence of, hemorrhage of the vasculature within the CNS of these mutants.

Adult *itgβ8 nestin-cre* mutants lack hemorrhages

Because *itgβ8*-null animals die before or shortly after birth, we used our conditional *itgβ8*-floxed allele to look at phenotypes in adult mutants. Adult *itgβ8 nestin-cre* mutants were examined 6–10 weeks after birth by Nissl stain (Fig. 6). Similar to control animals, this mutant showed no sign of cortical or thalamic hemorrhage compared with controls ($n = 6$) (Fig. 6*D*,*E*). Additionally, no cortical lamination defect was observed (Fig. 6*F*), which was not surprising, because radial glial attachment to the pial surface did not appear altered in the mutants during development. This suggests that the cerebrovascular defects observed in these animals at P0 were transient and were later repaired. The repair of the vascular defects observed at P0, however, was unexpected, because no *itgβ8*-null animal survived more than a few days postnatally.

Discussion

We generated a floxed allele of *itgβ8* to examine the functions of integrins containing the β8 subunit in the CNS. Targeted deletion of *itgβ8* from the embryonic neuroepithelium causes abnormal vascular development resulting in cerebral hemorrhage. Ablation of *itgβ8* from embryonic endothelial cells or neurons does not result in abnormal development of the brain vasculature. Expression of integrins containing the β8 subunit appears to be required on non-neuronal cells within the neuroepithelium for proper blood vessel development in the CNS. Moreover, neuroepithelial-derived astroglia lacking *itgβ8* are disorganized, particularly in relation to the vasculature within the forebrain. These findings complement our previous work

on *itgβ8*-null mice and further define the cell types that must express β8 within the CNS to promote normal vascular development during embryogenesis. In addition, adult animals lacking *itgβ8* in cells generated within the neuroepithelium did not have intracerebral hemorrhages, although hemorrhages occurred earlier during development. This result indicates that *itgβ8* is not required postnatally for proper cerebral blood vessel function.

Comparison of *itgβ8*-null mutants to conditional *itgβ8 nestin-cre* mutants

All *itgβ8*-null animals that survive gestation die within hours after birth with severe cerebral hemorrhage throughout the forebrain. Although *itgβ8 nestin-cre* mutants also show widespread cortical hemorrhage the day of birth, the hemorrhage is not as severe as in *itgβ8*-null animals and they survive birth to become adults. This marked difference may be a result of several possibilities. First, the complete *itgβ8*-null animals may develop under abnormal environmental conditions, such as hypoxia-induced oxidative stress, because *itgβ8* is required for proper vascular development of the placenta (Zhu et al., 2002).These environmental stress factor(s) may contribute indirectly by inducing cell death and brain tissue damage to increase the severity of hemorrhage in this mutant. Second, *nestin-cre* may have a slightly mosaic spatial expression pattern that prevents recombination of 100% of all neuroepithelial cells. The presence of a few cells that express β8 may reduce the severity of the hemorrhage observed at P0. Additionally, if *itgβ8* mRNA is produced before the onset of cre expression (and thus *itgβ8* deletion), enough β8 protein may be made to initiate aspects of proper vascular development. This latter possibility seems unlikely because the *nescre8* mutant has a very similar phenotype to that of the neural-specific *nestin-cre* mutant used in the bulk of our analyses but expresses cre 2 d earlier (Petersen et al., 2002).

CNS function of integrin αvβ8

Null alleles and floxed alleles of *itgβ8* and *itgαv* have been generated to elucidate the function of these integrin subunits *in vivo*. Null alleles of both *itgαv* and *itgβ8* have two stages of lethality, with a majority of each mutant dying during embryogenesis and a minority surviving until birth with severe cerebral hemorrhage (Bader et al., 1998; McCarty et al., 2002; Zhu et al., 2002). This evidence strongly suggests that these two subunits function together as a heterodimer during CNS vascular development. Indeed, αv and β8 may function exclusively together during vascular development, because no vascular defects were observed in *itgβ3/itgβ5* double knock-out mice (McCarty et al., 2002), *itgβ6* knock-out mice (Huang et al., 1996), or *nestin-cre*-derived *itgβ1*-deficient mice (Graus-Porta et al., 2001).

Both floxed alleles of *itgβ8* and *itgαv* have been crossed to *nestin-cre* and *tie2-cre* (Fig. 1, Fig 2) (McCarty et al., 2005; present study). Neither mutant obtained from the *tie2-cre* cross developed cerebral hemorrhage. Similarly, both mutants derived from the *nestin-cre* cross developed bilateral hemorrhage similar to, but less severe than, either null mutant. Our current study further defines non-neuronal cell types within the neuroepithelium responsible for proper capillary development within the CNS (Fig. 3). Moreover, our observation that astroglia in the *itgβ8 nestincre* mutant are disorganized (Fig. 5) implies that αvβ8 expressed on glial cell processes facilitates proper CNS blood vessel development. Cre expression driven by a glial lineage-specific promoter early during development would strengthen these findings; however, this may not be possible, because radial glia differentiate to form both glial cells and neurons (Doetsch, 2003). The *itgαv*-floxed mice were crossed to mice expressing cre driven by the human *GFAP* promoter (*hGFAP*) in an attempt to recombine primarily CNS glia originating from *GFAP*-positive radial glia. The resulting mutants, however, developed only a mild cerebral hemorrhage, most likely attributable to the late onset (~E15) of cre expression (McCarty et al., 2005). Although *GFAP*-positive radial glia are known to give rise to astrocytes and other glial cell types, almost all cortical projection neurons, and some striatal neurons, also originate from this radial glial lineage (Doetsch, 2003). At least some of these neurons are also

likely to have lost *itgαv* as a result of recombination mediated by *hGFAP-cre*; thus, they may contribute to any hemorrhage observed in this mutant. Our observation that *itgβ8 nex-cre* mutants do not develop cerebral hemorrhage (Fig. 3) indicates that cortical neurons do not contribute to the cerebral hemorrhage observed in *itgβ8 nestin-cre* mutants or *itgβ8*-null animals at P0. Together, this evidence suggests that deletion of αvβ8 on glial cells within the neuroepithelium is responsible for the hemorrhage observed in the *itgβ8*- and *itgαv*-null animals.

Because neither the *itgαv*- or *itgβ8*-null animals survive long after birth, use of the floxed *itgβ8* allele has enabled investigation of the postnatal functions of β8. Surprisingly, we discovered that adult *itgβ8 nestin-cre* mutants do not have cerebral hemorrhage (Fig. 6). Although a majority of *itgαv nestin-cre* mutants also survive neonatal hemorrhage to become mature adults, a few do not fully repair the hemorrhage and die within a few weeks after birth (McCarty et al., 2005). The absence of premature death in *itgβ8 nestin-cre* mutants could reflect differences in the background strains of these two mutants. Lastly, *itgβ8 nestin-cre* mutant animals begin to display abnormal gait in the hind limbs 8 weeks after birth (J. M. Proctor and L. F. Reichardt, unpublished observations). Although we are currently investigating this adult phenotype in more detail, it is worth noting that adult *itgαv nestin-cre* mutants also display abnormal gait with a similar time of onset (McCarty et al., 2005).

Brain vascular development and integrin αvβ8

The cerebral hemorrhage observed in the conditional *itgβ8 nestin-cre* mutants suggests a severe defect in vascular development and function. Analysis of mutant brains revealed aberrant capillary vessel morphology and abnormal clustering of endothelial cells (Fig. 4). However, vessels maintained an intact basement membrane and normal endothelial cell-associated pericytes (Fig. 4). The defect in glial alignment and possible lack of association with endothelial cells observed in the *itgβ8 nestin-cre* mutants (Fig. 5) suggest that αvβ8 regulates vascular morphogenesis through its expression on neuroepithelial cells, particularly glia. These data support a model in which αvβ8 adheres to ligand(s) within the extracellular matrix or ligand (s) expressed directly in brain capillary vessels to mediate glial cell– endothelial cell contact. This contact could provide instructive cues for proper vascular morphogenesis during early development and physical support during later aspects of CNS development. None of the known ligands for αvβ8, however, are required for vascular development of the CNS. For example, one-half of TGF-β1-deficient mice have a defective yolk sac vasculature, but the remaining one-half survive birth with no sign of cerebral hemorrhage and die because of a multifocal inflammatory disorder (Shull et al., 1992;Dickson et al., 1995). Knock-out mice of ECM ligands such as vitronectin develop normally and are fertile (Zheng et al., 1995). None of the laminin isoform knock-out mice develop cerebral hemorrhage (Li et al., 2003), although laminin-α5-deficient mice have a defective placental vasculature (Miner et al., 1998). Lastly, collagen IV-deficient mice die at midgestation, but the capillary networks of the embryo, yolk sac, and placenta appear normal (Poschl et al., 2004). Together, these data suggest that the αvβ8 ligand responsible for its regulatory function in CNS vasculature development has not been identified.

Strikingly similar to *itgβ8*-null mice, total deletion of *neuropilin-1* (*npn-1*) results in defective yolk sac and cerebral vessel development and early embryonic death (Kawasaki et al., 1999). Neuropilin-1 is a known receptor for the $VEGF_{165}$ isoform of VEGF-A (Breier et al., 1992; Soker et al., 1998). One putative mechanism by which αvβ8 expressed on glial cells could regulate vascular development is by indirectly regulating release of secreted factors, such as VEGF, through cross talk with endothelial cell receptors such as neuropilin-1. The $VEGF_{165}$ binding site on neuropilin-1 has been shown to be necessary for proper capillary development in the embryonic mouse brain (Gu et al., 2003). Additionally, *npn-1* mutants display aberrant

endothelial cell clusters (Gerhardt et al., 2004) similar to those observed in the *itgβ8*-null and *nestin-cre* mutants. Increased capillary permeability and endothelial cell hyperproliferation are known effects of augmented VEGF expression (Cheng et al., 1997; Sundberg et al., 2001; Gora-Kupilas and Josko, 2005). Bromodeoxyuridine labeling of endothelial cells in the *itgβ8*-null animals demonstrates that these cells are in fact hyperproliferative in this mutant (Zhu et al., 2002). Through possible communication with neuropilin-1, αvβ8 may regulate expression or secretion of specific isoforms of VEGF, such as $VEGF_{165}$, and thereby regulate vascular morphogenesis. Other molecules such as Eph receptors and semaphorins have been shown to interact with integrins and their signaling pathways (Zou et al., 1999; Pasterkamp et al., 2003; Serini et al., 2003) and thus may also play a role in regulating vascular development of the brain. We are currently pursuing the mechanism by which αvβ8 functions in the developing mouse brain.

Our current study defines neuroepithelial cells and glia as the primary cell types in which *itgβ8* expression is essential for proper development of capillary growth in the embryonic brain. It is essential now to identify the ligand(s) for αvβ8 in the CNS and to develop reagents that will facilitate our understanding of the mechanism by which αvβ8 promotes proper vascular development. Use of the *itgβ8*-floxed allele in elucidating the signaling pathways through which integrin αvβ8 functions should help define the regulatory mechanisms necessary to establish an organized capillary network in the developing brain.

Supplementary Material

Refer to Web version on PubMed Central for supplementary material.

Acknowledgments

This work was supported by National Institutes of Health Grant R01-NS19090 (L.F.R). J.M.P. is the recipient of a predoctoral fellowship from the National Science Foundation. L.F.R. is an investigator of the Howard Hughes Medical Institute. We thank Klaus-Armin Nave for the *nex-cre* mice, Zhen Huang, James Linton, and Ben Cheyette for critical reading of this manuscript, and members of the Reichardt Laboratory for helpful discussions. The RC2 antibody, developed by Miyuki Yamamoto, was obtained from the Developmental Studies Hybridoma Bank developed under the auspices of the National Institute of Child Health and Human Development and maintained by the Department of Biological Sciences, The University of Iowa (Iowa City, IA).

References

Abbott NJ, Romero IA. Transporting therapeutics across the blood-brain barrier. Mol Med Today 1996;2:106–113. [PubMed: 8796867]

Bader BL, Rayburn H, Crowley D, Hynes RO. Extensive vasculogenesis, angiogenesis, and organogenesis precede lethality in mice lacking all alpha v integrins. Cell 1998;95:507–519. [PubMed: 9827803]

Beggs HE, Schahin-Reed D, Zang K, Goebbels S, Nave KA, Gorski J, Jones KR, Sretavan D, Reichardt LF. FAK deficiency in cells contributing to the basal lamina results in cortical abnormalities resembling congenital muscular dystrophies. Neuron 2003;40:501–514. [PubMed: 14642275]

Breier G, Albrecht U, Sterrer S, Risau W. Expression of vascular endothelial growth factor during embryonic angiogenesis and endothelial cell differentiation. Development 1992;114:521–532. [PubMed: 1592003]

Brockschnieder D, Lappe-Siefke C, Goebbels S, Boesl MR, Nave KA, Riethmacher D. Cell depletion due to diphtheria toxin fragment A after Cre-mediated recombination. Mol Cell Biol 2004;24:7636–7642. [PubMed: 15314171]

Calderwood DA. Integrin activation. J Cell Sci 2004;117:657–666. [PubMed: 14754902]

Cheng SY, Nagane M, Huang HS, Cavenee WK. Intracerebral tumor associated hemorrhage caused by overexpression of the vascular endothelial growth factor isoforms VEGF121 and VEGF165 but not VEGF189. Proc Natl Acad Sci USA 1997;94:12081–12087. [PubMed: 9342366]

Dickson MC, Martin JS, Cousins FM, Kulkarni AB, Karlsson S, Akhurst RJ. Defective haematopoiesis and vasculogenesis in transforming growth factor-beta 1 knock out mice. Development 1995;121:1845–1854. [PubMed: 7600998]

Doetsch F. The glial identity of neural stem cells. Nat Neurosci 2003;6:1127–1134. [PubMed: 14583753]

Engelhardt B. Development of the blood-brain barrier. Cell Tissue Res 2003;314:119–129. [PubMed: 12955493]

Gerhardt H, Golding M, Fruttiger M, Ruhrberg C, Lundkvist A, Abramsson A, Jeltsch M, Mitchell C, Alitalo K, Shima D, Betsholtz C. VEGF guides angiogenic sprouting utilizing endothelial tip cell filopodia. J Cell Biol 2003;161:1163–1177. [PubMed: 12810700]

Gerhardt H, Ruhrberg C, Abramsson A, Fujisawa H, Shima D, Betsholtz C. Neuropilin-1 is required for endothelial tip cell guidance in the developing central nervous system. Dev Dyn 2004;231:503–509. [PubMed: 15376331]

Gora-Kupilas K, Josko J. The neuroprotective function of vascular endothelial growth factor (VEGF). Folia Neuropathol 2005;43:31–39. [PubMed: 15827888]

Graus-Porta D, Blaess S, Senften M, Littlewood-Evans A, Damsky C, Huang Z, Orban P, Klein R, Schittny JC, Muller U. Beta1-class integrins regulate the development of laminae and folia in the cerebral and cerebellar cortex. Neuron 2001;31:367–379. [PubMed: 11516395]

Green LJ, Mould AP, Humphries MJ. The integrin beta subunit. Int J Biochem Cell Biol 1998;30:179–184. [PubMed: 9608671]

Gu C, Rodriguez ER, Reimert DV, Shu T, Fritzsch B, Richards LJ, Kolodkin AL, Ginty DD. Neuropilin-1 conveys semaphorin and VEGF signaling during neural and cardiovascular development. Dev Cell 2003;5:45–57. [PubMed: 12852851]

Hirsch E, Gullberg D, Balzac F, Altruda F, Silengo L, Tarone G. Alpha v integrin subunit is predominantly located in nervous tissue and skeletal muscle during mouse development. Dev Dyn 1994;201:108–120. [PubMed: 7873784]

Huang XZ, Wu JF, Cass D, Erle DJ, Corry D, Young SG, Farese RV Jr, Sheppard D. Inactivation of the integrin beta 6 subunit gene reveals a role of epithelial integrins in regulating inflammation in the lung and skin. J Cell Biol 1996;133:921–928. [PubMed: 8666675]

Kacem K, Lacombe P, Seylaz J, Bonvento G. Structural organization of the perivascular astrocyte endfeet and their relationship with the endothelial glucose transporter: a confocal microscopy study. Glia 1998;23:1–10. [PubMed: 9562180]

Kawasaki T, Kitsukawa T, Bekku Y, Matsuda Y, Sanbo M, Yagi T, Fujisawa H. A requirement for neuropilin-1 in embryonic vessel formation. Development 1999;126:4895–4902. [PubMed: 10518505]

Lewandoski M, Meyers EN, Martin GR. Analysis of Fgf8 gene function in vertebrate development. Cold Spring Harb Symp Quant Biol 1997;62:159–168. [PubMed: 9598348]

Li S, Edgar D, Fassler R, Wadsworth W, Yurchenco PD. The role of laminin in embryonic cell polarization and tissue organization. Dev Cell 2003;4:613–624. [PubMed: 12737798]

McCarty JH, Monahan-Earley RA, Brown LF, Keller M, Gerhardt H, Rubin K, Shani M, Dvorak HF, Wolburg H, Bader BL, Dvorak AM, Hynes RO. Defective associations between blood vessels and brain parenchyma lead to cerebral hemorrhage in mice lacking alphav integrins. Mol Cell Biol 2002;22:7667–7677. [PubMed: 12370313]

McCarty JH, Lacy-Hulbert A, Charest A, Bronson RT, Crowley D, Housman D, Savill J, Roes J, Hynes RO. Selective ablation of αv integrins in the central nervous system leads to cerebral hemorrhage, seizures, axonal degeneration and premature death. Development 2005;132:165–176. [PubMed: 15576410]

Mendell JT, Sharifi NA, Meyers JL, Martinez-Murillo F, Dietz HC. Nonsense surveillance regulates expression of diverse classes of mammalian transcripts and mutes genomic noise. Nat Genet 2004;36:1073–1078. [PubMed: 15448691]

Milner R, Frost E, Nishimura S, Delcommenne M, Streuli C, Pytela R, Ffrench-Constant C. Expression of alpha vbeta3 and alpha vbeta8 integrins during oligodendrocyte precursor differentiation in the presence and absence of axons. Glia 1997;21:350–360. [PubMed: 9419010]

Miner JH, Cunningham J, Sanes JR. Roles for laminin in embryogenesis: exencephaly, syndactyly, and placentopathy in mice lacking the laminin alpha5 chain. J Cell Biol 1998;143:1713–1723. [PubMed: 9852162]

Misson JP, Edwards MA, Yamamoto M, Caviness VS Jr. Identification of radial glial cells within the developing murine central nervous system: studies based upon a new immunohistochemical marker. Brain Res Dev Brain Res 1988;44:95–108.

Moyle M, Napier MA, McLean JW. Cloning and expression of a divergent integrin subunit beta 8. J Biol Chem 1991;266:19650–19658. [PubMed: 1918072]

Mu D, Cambier S, Fjellbirkeland L, Baron JL, Munger JS, Kawakatsu H, Sheppard D, Broaddus VC, Nishimura SL. The integrin alpha(v) beta8 mediates epithelial homeostasis through MT1-MMP-dependent activation of TGF-beta1. J Cell Biol 2002;157:493–507. [PubMed: 11970960]

Nishimura SL, Sheppard D, Pytela R. Integrin alpha v beta 8. Interaction with vitronectin and functional divergence of the beta 8 cytoplasmic domain. J Biol Chem 1994;269:28708–28715. [PubMed: 7525578]

Nishimura SL, Boylen KP, Einheber S, Milner TA, Ramos DM, Pytela R. Synaptic and glial localization of the integrin alphavbeta8 in mouse and rat brain. Brain Res 1998;791:271–282. [PubMed: 9593935]

Park JA, Choi KS, Kim SY, Kim KW. Coordinated interaction of the vascular and nervous systems: from molecule- to cell-based approaches. Biochem Biophys Res Commun 2003;311:247–253. [PubMed: 14592405]

Pasterkamp RJ, Peschon JJ, Spriggs MK, Kolodkin AL. Semaphorin 7A promotes axon outgrowth through integrins and MAPKs. Nature 2003;424:398–405. [PubMed: 12879062]

Petersen PH, Zou K, Hwang JK, Jan YN, Zhong W. Progenitor cell maintenance requires numb and numblike during mouse neurogenesis. Nature 2002;419:929–934. [PubMed: 12410312]

Pinkstaff JK, Detterich J, Lynch G, Gall C. Integrin subunit gene expression is regionally differentiated in adult brain. J Neurosci 1999;19:1541–1556. [PubMed: 10024342]

Poschl E, Schlotzer-Schrehardt U, Brachvogel B, Saito K, Ninomiya Y, Mayer U. Collagen IV is essential for basement membrane stability but dispensable for initiation of its assembly during early development. Development 2004;131:1619–1628. [PubMed: 14998921]

Rodriguez CI, Buchholz F, Galloway J, Sequerra R, Kasper J, Ayala R, Stewart AF, Dymecki SM. High-efficiency deleter mice show that FLPe is an alternative to Cre-loxP. Nat Genet 2000;25:139–140. [PubMed: 10835623]

Ruhrberg C, Gerhardt H, Golding M, Watson R, Ioannidou S, Fujisawa H, Betsholtz C, Shima DT. Spatially restricted patterning cues provided by heparin-binding VEGF-A control blood vessel branching morphogenesis. Genes Dev 2002;16:2684–2698. [PubMed: 12381667]

Serini G, Valdembri D, Zanivan S, Morterra G, Burkhardt C, Caccavari F, Zammataro L, Primo L, Tamagnone L, Logan M, Tessier-Lavigne M, Taniguchi M, Puschel AW, Bussolino F. Class 3 semaphorins control vascular morphogenesis by inhibiting integrin function. Nature 2003;424:391–397. [PubMed: 12879061]

Shull MM, Ormsby I, Kier AB, Pawlowski S, Diebold RJ, Yin M, Allen R, Sidman C, Proetzel G, Calvin D, Annunziata N, Doetschman T. Targeted disruption of the mouse transforming growth factor-beta 1 gene results in multifocal inflammatory disease. Nature 1992;359:693–699. [PubMed: 1436033]

Simard M, Arcuino G, Takano T, Liu QS, Nedergaard M. Signaling at the gliovascular interface. J Neurosci 2003;23:9254–9262. [PubMed: 14534260]

Soker S, Takashima S, Miao HQ, Neufeld G, Klagsbrun M. Neuropilin-1 is expressed by endothelial and tumor cells as an isoform-specific receptor for vascular endothelial growth factor. Cell 1998;92:735–745. [PubMed: 9529250]

Sundberg C, Nagy JA, Brown LF, Feng D, Eckelhoefer IA, Manseau EJ, Dvorak AM, Dvorak HF. Glomeruloid microvascular proliferation follows adenoviral vascular permeability factor/vascular endothelial growth factor-164 gene delivery. Am J Pathol 2001;158:1145–1160. [PubMed: 11238063]

Tronche F, Kellendonk C, Kretz O, Gass P, Anlag K, Orban PC, Bock R, Klein R, Schutz G. Disruption of the glucocorticoid receptor gene in the nervous system results in reduced anxiety. Nat Genet 1999;23:99–103. [PubMed: 10471508]

Tuckwell DS, Humphries MJ. A structure prediction for the ligand-binding region of the integrin beta subunit: evidence for the presence of a von Willebrand factor A domain. FEBS Lett 1997;400:297–303. [PubMed: 9009218]

Venstrom K, Reichardt L. Beta 8 integrins mediate interactions of chick sensory neurons with laminin-1, collagen IV, and fibronectin. Mol Biol Cell 1995;6:419–431. [PubMed: 7542940]

Xiong JP, Stehle T, Diefenbach B, Zhang R, Dunker R, Scott DL, Joachimiak A, Goodman SL, Arnaout MA. Crystal structure of the extracellular segment of integrin alpha Vbeta3. Science 2001;294:339–345. [PubMed: 11546839]

Yancopoulos GD, Davis S, Gale NW, Rudge JS, Wiegand SJ, Holash J. Vascular-specific growth factors and blood vessel formation. Nature 2000;407:242–248. [PubMed: 11001067]

Zheng X, Saunders TL, Camper SA, Samuelson LC, Ginsburg D. Vitronectin is not essential for normal mammalian development and fertility. Proc Natl Acad Sci USA 1995;92:12426–12430. [PubMed: 8618914]

Zhu J, Motejlek K, Wang D, Zang K, Schmidt A, Reichardt LF. beta8 integrins are required for vascular morphogenesis in mouse embryos. Development 2002;129:2891–2903. [PubMed: 12050137]

Zou JX, Wang B, Kalo MS, Zisch AH, Pasquale EB, Ruoslahti E. An Eph receptor regulates integrin activity through R-Ras. Proc Natl Acad Sci USA 1999;96:13813–13818. [PubMed: 10570155]

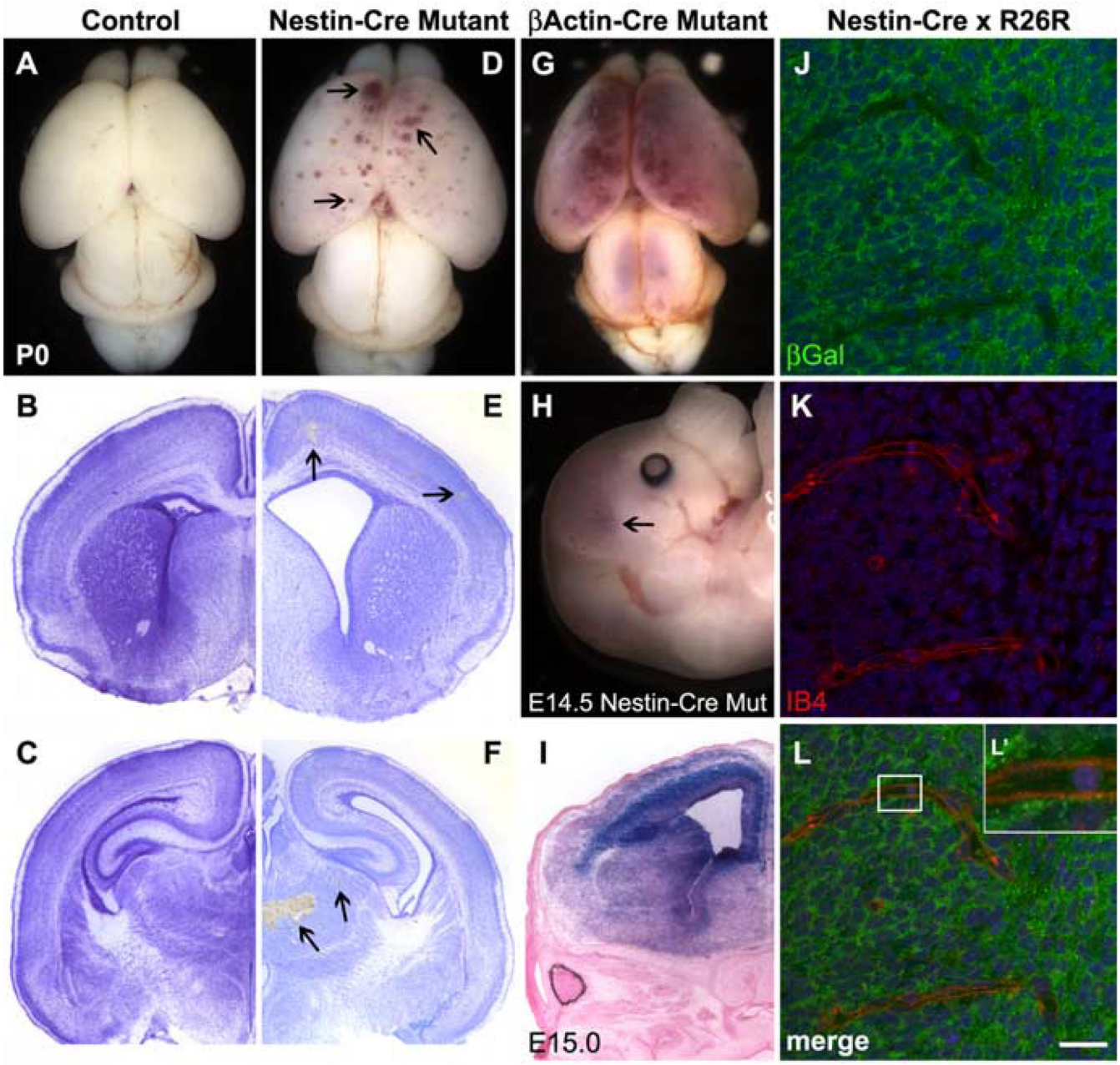

Figure 1.

Phenotypic defects observed after conditional deletion of *itgβ8* from the neuroepithelium using *nestin-cre*. ***A***, Wild-type brain from P0 neonate. ***B, C***, Nissl-stained sections of a control brain. ***D***, P0 brain lacking *itgβ8* because of conditional deletion mediated by neuroepithelial-specific *nestin-cre*. Note the blood produced from hemorrhages throughout the dorsal and rostral cortices (arrowheads). ***E, F***, Nissl-stained sections of a *nestin-cre* mutant brain. Notice the hemorrhages (arrowheads) throughout the cortex (***E***) in addition to the massive hemorrhage in the thalamus (***F***). ***G***, P0 mutant animal generated using the β-*actin-cre* line. Mutants generated with this *cre* line display phenotypes not obviously different from the null animal. An avascularized yolk sac and placenta is seen in the majority of embryos that die by E11.5, and severe hemorrhage is seen in the brain of embryos that survive to birth. ***H***, E14.5 brain lacking

itgβ8 from the neuroepithelium because of conditional deletion mediated by neuroepithelial-specific *nestin-cre*. Note the blood produced from hemorrhages throughout the dorsal and rostral cortices (arrowhead). ***I***, LacZ-stained section from an E15 *nestin-cre*-positive animal crossed to the R26R reporter strain. Note that the neuroepithelium is almost entirely recombined. ***J–L′***, β-galactosidase expression analysis of E15 embryo cortices (one-half day after hemorrhage was observed in *nestin-cre* mutants) obtained from a cross of a *nestin-cre*-positive animal and the R26R reporter line. Note the strong expression of β-galactosidase (green) in cells of the neuroepithelium but the lack of β-galactosidase immunolabeling of the endothelial cells labeled with isolectin B4 (red) (***L′***). Cell nuclei were counterstained with TO-PRO-3 (blue).βGal, β-Galactosidase; Mut, mutant; IB4, isolectin B4. Scale bar: ***L***, 20 μm.

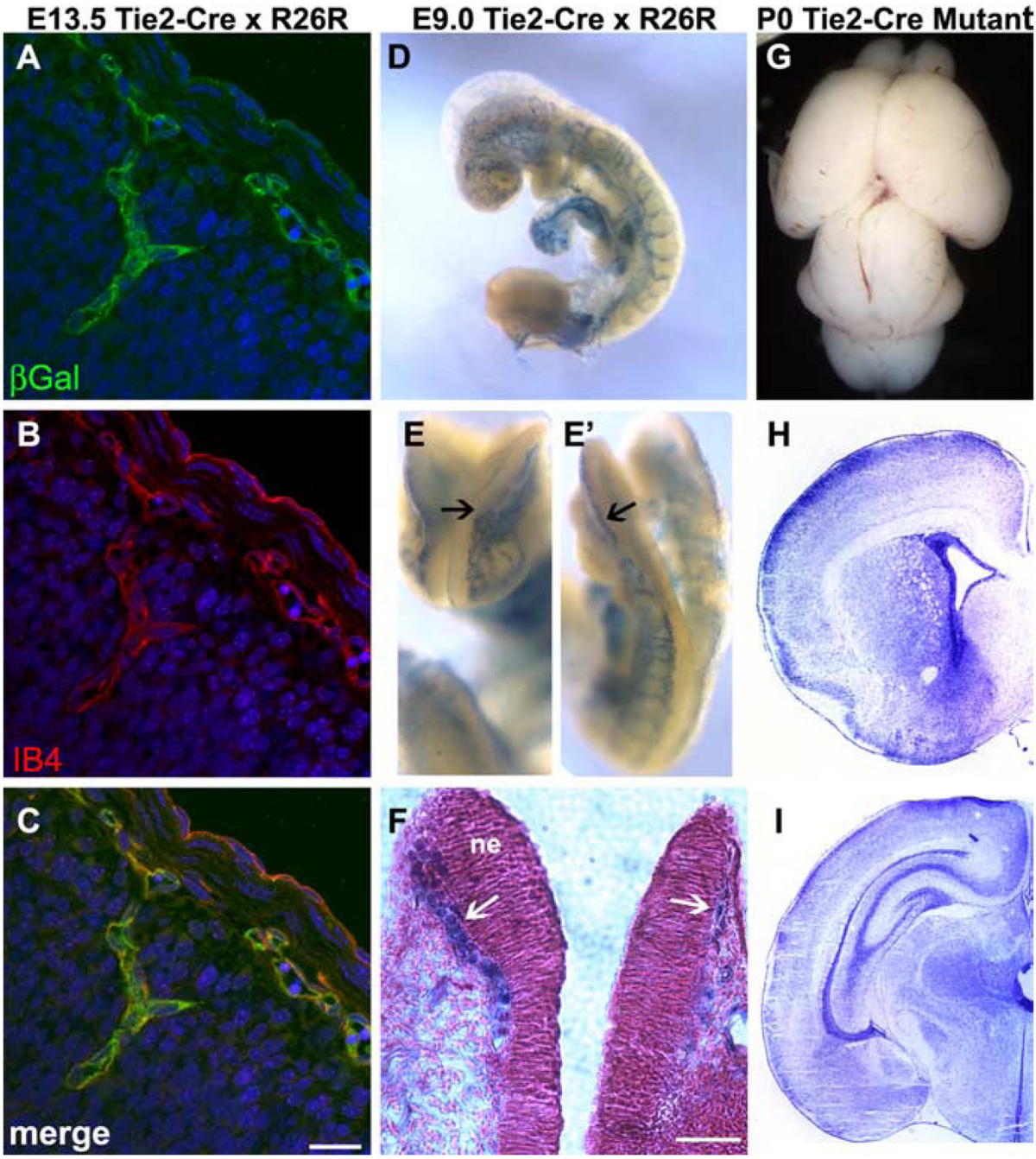

Figure 2.

Conditional deletion of *itgβ8* from vascular endothelial cells using *tie2-cre* does not result in cerebral hemorrhage. ***A–C***, β-Galactosidase (βGal) expression analysis of E13.5 embryo cortices obtained from a cross between a *tie2-cre*-positive animal and the R26R reporter line. Note that β-galactosidase (green) expression is very strong and perfectly overlaps with the isolectin B4 (IB4) (red) (***B, C***) immunolabeling of endothelial cells. Cell nuclei were counterstained with TO-PRO-3 (blue).***D–F***, LacZ reporter analysis of E9 embryos obtained from a cross between a *tie2-cre*-positive animal and the R26R reporter line. Notice that cre-mediated recombination is very strong in the head vasculature before invasion of the neuroepithelium (***E, E′***, arrows). ***F***, Coronal slice of embryo from ***E***, counterstained with

Nuclear Fast Red. Notice that LacZ-positive vessels (blue) have not yet invaded the neuroepithelium (ne) at 9.0 d postconception. ***G***, P0 brain lacking *itgβ8* in vascular endothelial cells because of conditional deletion mediated by *tie2-cre*. ***H, I***, Nissl-stained sections of a *tie2-cre* mutant P0 brain. Note the absence of hemorrhage. Scale bars: ***C***, 20 μm; ***F***, 40 μm.

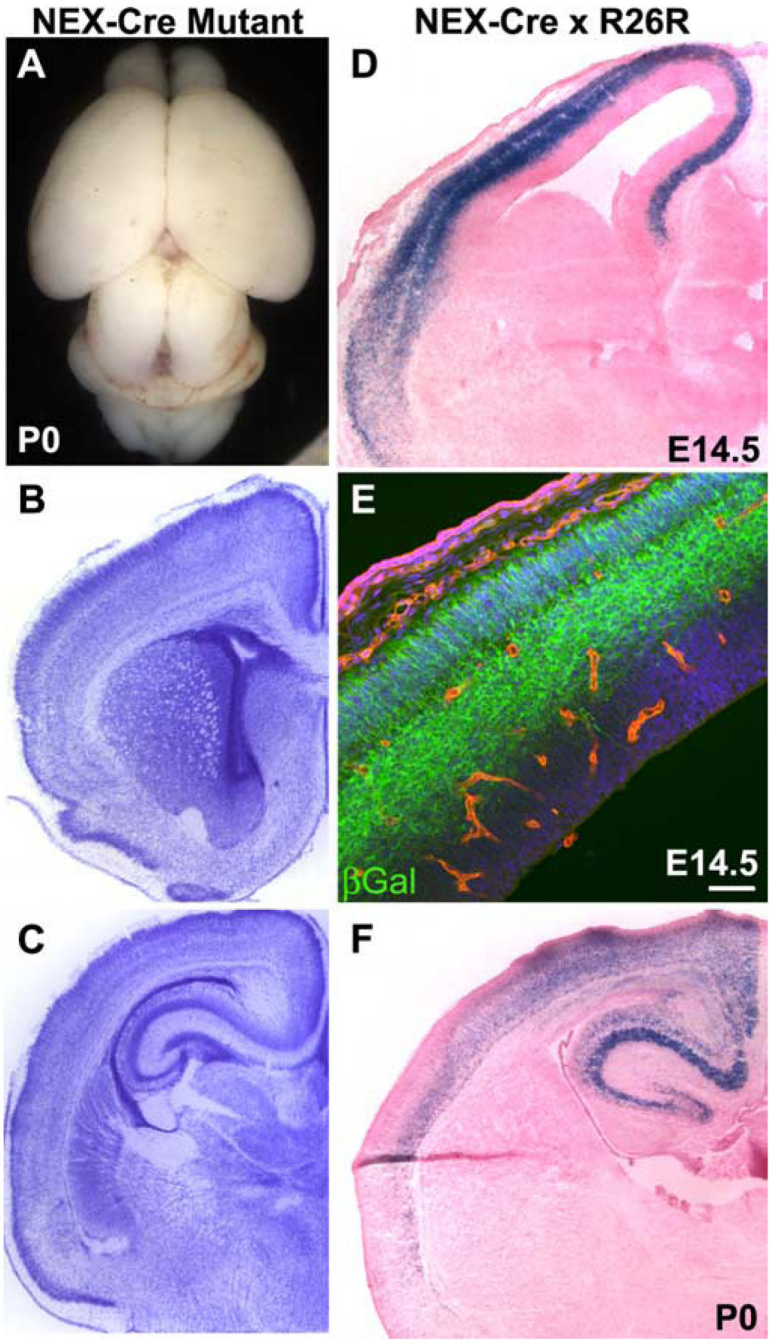

Figure 3.

Conditional deletion of *itgβ8* from postmitotic neurons using *nex-cre* does not result in cerebral hemorrhage. ***A***, P0 brain lacking *itgβ8* in postmitotic neurons because of conditional deletion mediated by *nex-cre*. ***B, C***, Nissl-stained sections of a *nex-cre* mutant P0 brain. ***D, F***, LacZ-stained sections from an E14.5 embryo cortex and P0 cortex obtained from a cross between a *nex-cre*-positive animal and the R26R reporter line. *Cre*-mediated recombination is very strong in the future cortical plate by E14.5 when hemorrhage is observed in the *nestin-cre* mutant and remains strong after birth. ***E***,β-Galactosidase (βGal) expression analysis of E14.5 embryo cortex. Note that βGal (green) immunolabeling is limited to cells within the future cortical

plate. Endothelial cells were immunolabeled with isolectin B4 (red) and were not recombined by this *cre* line. Cell nuclei were counterstained with TO-PRO-3 (blue). Scale bar: ***E***, 50 μm.

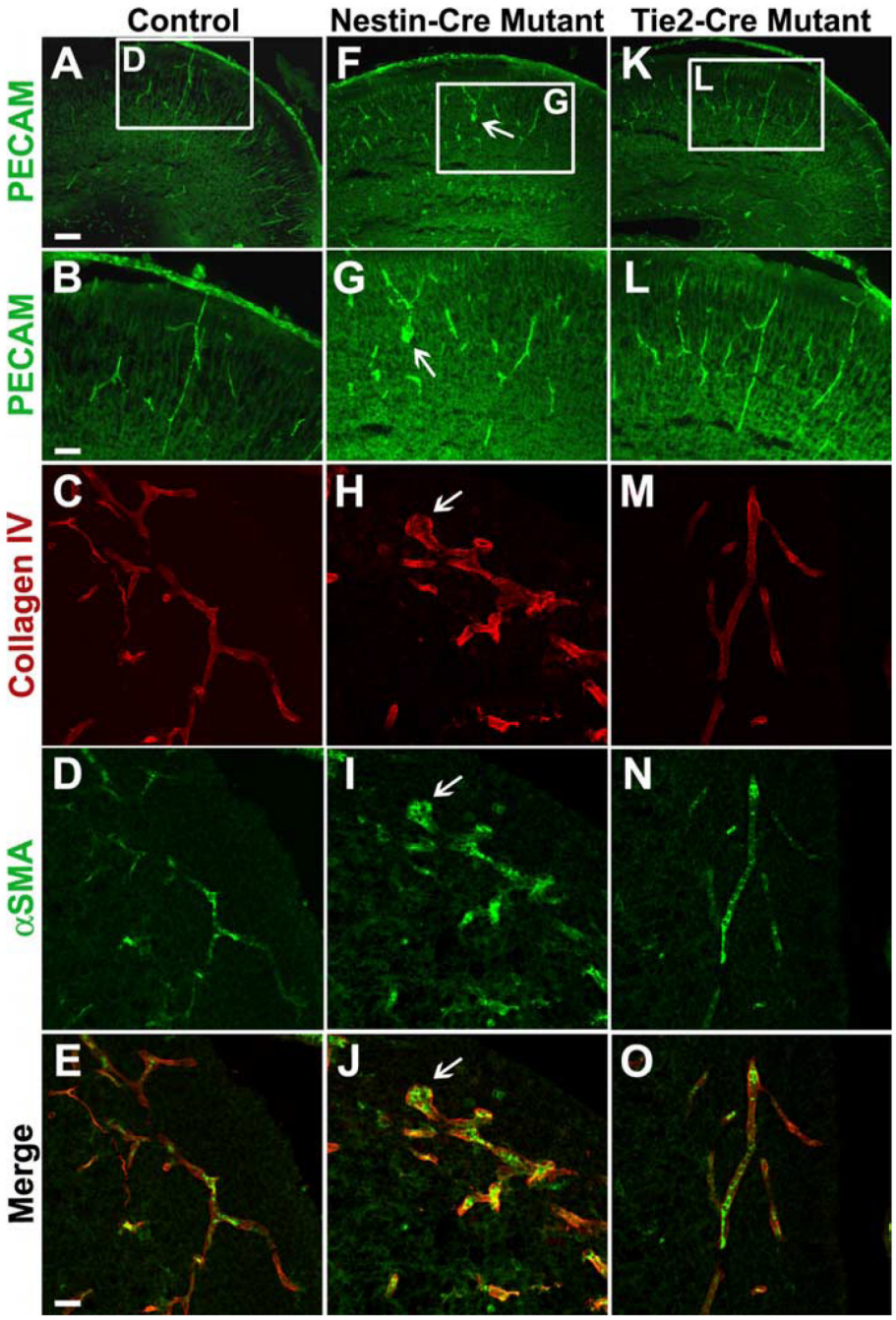

Figure 4.

Conditional deletion of *itgβ8* in the neuroepithelium leads to endothelial cell irregularities in the P0 neonatal cortex. Anti-PECAM immunolabeling of P0 coronal sections of the forebrain to visualize vascular endothelial cells is shown. ***A, B***, Control. ***F, G***, *Nestin-cre*-targeted mutant. ***K, L***, *Tie2-cre*-targeted mutant. Notice the bulbous organization of endothelial cell clusters in the cortex (arrows) of the *nestin-cre*-targeted mutant (***F, G***). Anti-collagen IV immunolabeling of P0 coronal sections of the neuroepithelium to visualize the basal lamina surrounding the vasculature is shown. ***C, E***, Control. ***H, J***, *Nestin-cre*-targeted mutant. ***M, O***, *Tie2-cre*-targeted mutant. Notice the intact basement membrane in the area of an endothelial cell cluster (arrowhead) in the *nestin-cre*-targeted mutant (***H, J***). Anti-α-smooth muscle actin (αSMA)

immunolabeling of pericytes in P0 coronal sections of the neuroepithelium. ***D, E***, Control. ***I, J***, *Nestin-cre* mutant. ***N, O***, *Tie2-cre* mutant. Note the normal recruitment of pericytes to the vasculature in both mutants. Scale bars: ***A***, 80 μm; ***B, E***, 40 μm.

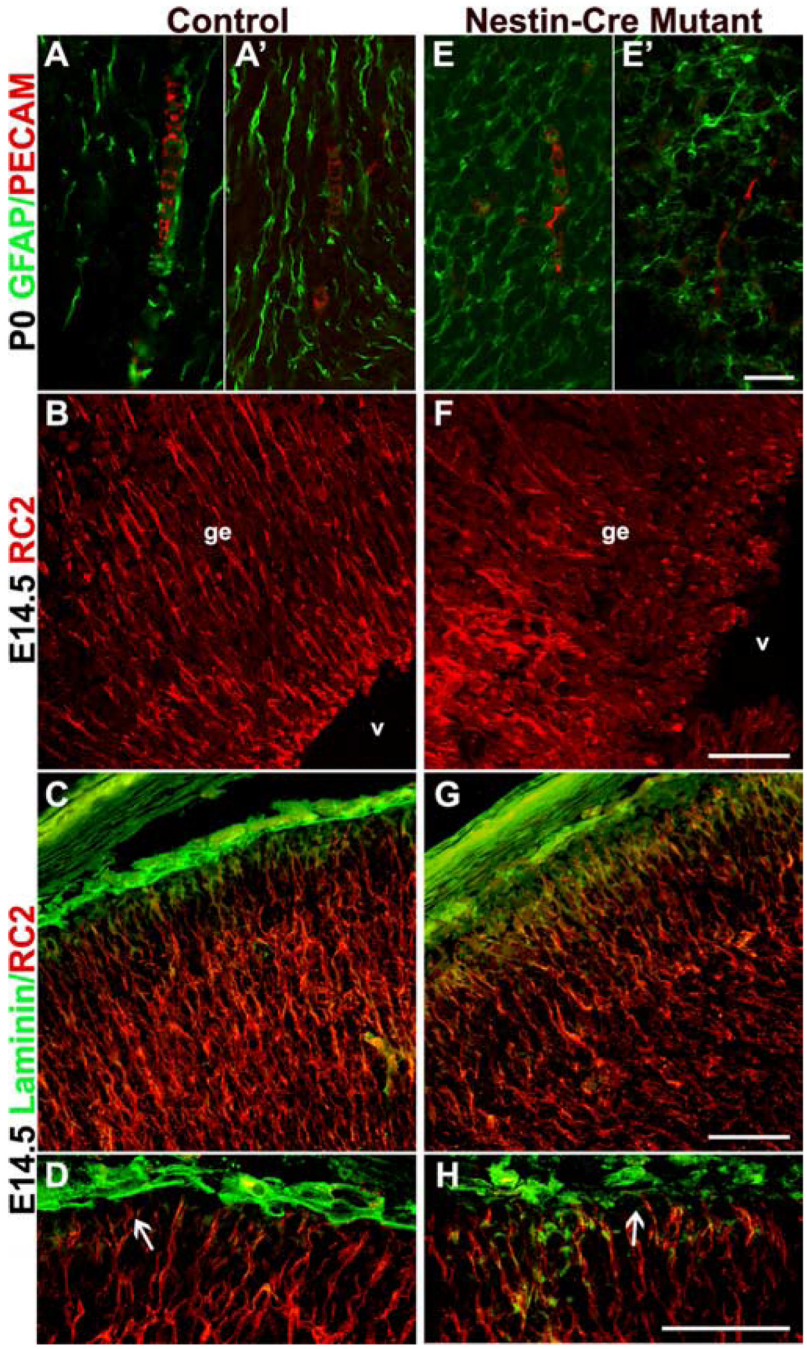

Figure 5.

Itgβ8 nestin-cre mutants have abnormally organized cortical glia. Anti-PECAM/GFAP immunostaining of endothelial cells and glia, respectively, in P0 coronal sections of the dorsal forebrain is shown. ***A, A′***, Control. ***E, E′***, *Nestin-cre* mutant. Notice the disorganization of the astroglia and the lack of alignment between endothelial cells and the astroglial processes (***E, E′***). Anti-RC2 immunostaining of radial glia in E14.5 coronal sections of the ganglionic eminence is shown. ***B***, Control. ***F***, *Nestin-cre*-targeted mutant. Radial glia in ***F*** are badly disorganized, most likely because of hemorrhage within the ganglionic eminence (ge) near the lateral ventricles (v). Anti-RC2 and anti-laminin immunolabeling of E14.5 coronal sections demonstrating radial glia cell morphology in cortices of a control animal (***C, D***) and a nestin-

cre mutant (***G, H***) is shown. Attachment of the radial glia to the pial surface in the *nestin-cre* mutant does not appear altered (***H***, arrow), and glial processes display normal organization. Scale bars: ***E′***, 20 μm; ***F–H***, 50 μm.

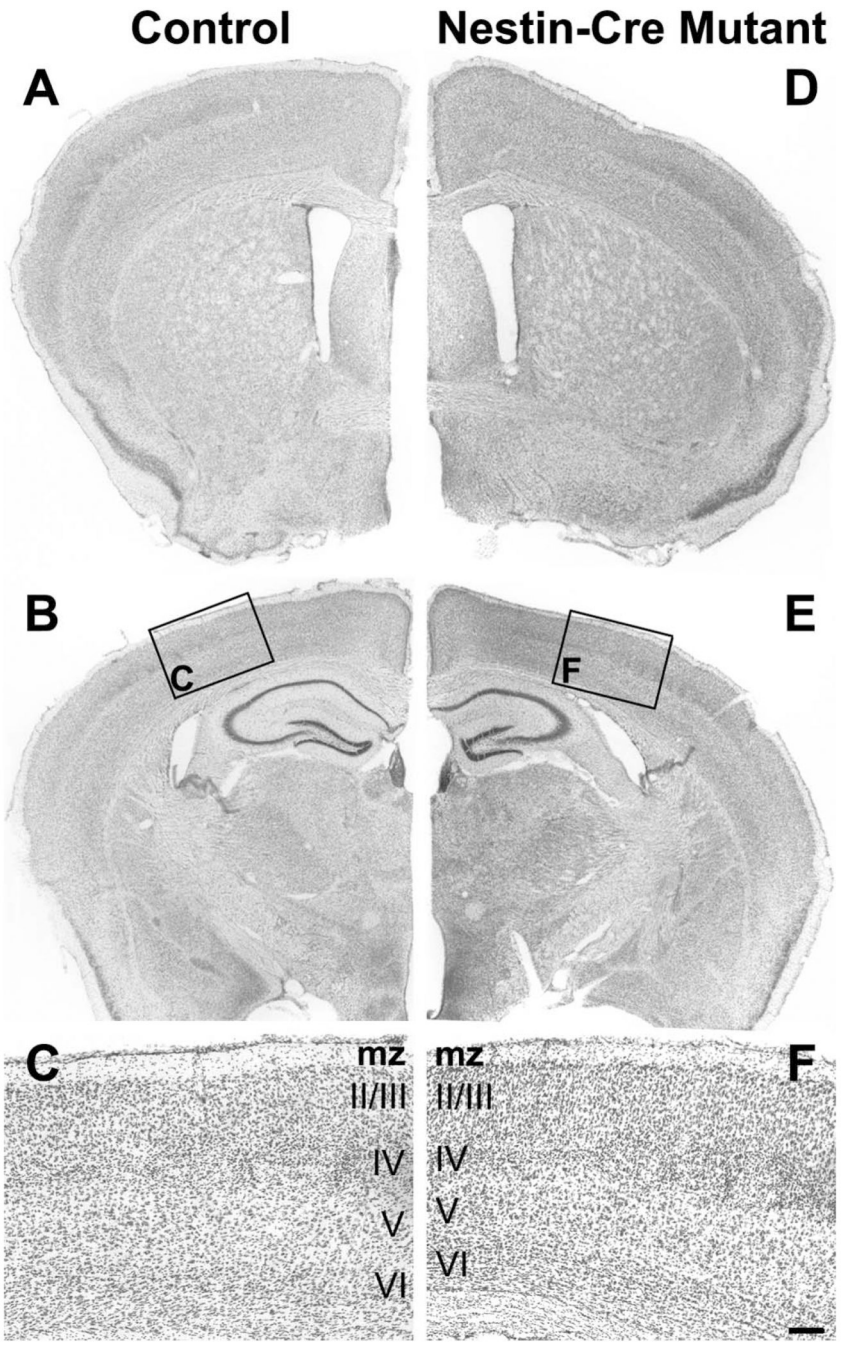

Figure 6.

Adult *itgβ8 nestin-cre* mutants show no sign of brain hemorrhage. ***A***, Six-week-old control. ***D***, Six-week-old *nestin-cre*-targeted mutant coronal sections at the level of the lateral ventricles in the forebrain stained with Nissl. ***B***, Control. ***E***, *Nestin-cre* mutant coronal sections at the level of the hippocampus stained with Nissl. Note the lack of hemorrhage or other obvious defect in the cortex or thalamus. ***C, F***, High magnification of cortical sections boxed in ***B*** and ***E***. All cortical layers are present and in the correct order in the mutant. mz, Marginal zone. Scale bar: ***F***, 100 μm.